

## Electroexcitation of $^{11}\text{B}^\dagger$

P. T. Kan, G. A. Peterson, and D. V. Webb

*Department of Physics and Astronomy, University of Massachusetts, Amherst, Massachusetts 01002*

S. P. Fivozinsky, J. W. Lightbody, Jr., and S. Penner

*Center for Radiation Research, National Bureau of Standards, Washington, D. C. 20234*

(Received 18 September 1974)

Electrons with incident energies between 52.3 and 90.0 MeV have been scattered from the nucleus of  $^{11}\text{B}$ . Spectra of scattered electrons corresponding to excitation energies up to 32 MeV were observed at angles of  $75^\circ$  and  $145^\circ$ . Form factors of the states at 2.12, 4.44, 5.02, 8.57, and 8.93 MeV, and of the continuum region up to 30 MeV, have been separated into longitudinal and transverse components. The  $^{11}\text{B}$  dipole giant resonance is smooth relative to those of  $^{12}\text{C}$  and  $^{13}\text{C}$ . A mixed  $M1$ - $E2$  transition was observed at 13.0 MeV and a broad transverse resonance, possibly magnetic, was seen at 15.5 MeV.

[ NUCLEAR REACTIONS  $^{11}\text{B}(e, e')$ ,  $E = 52.3$ – $90.0$  MeV,  $\theta = 75^\circ$ – $145^\circ$ ; measured  $\sigma(E', \theta)$ ; deduced  $B(E2)$ ,  $B(M1)$ , giant resonance differential form factors. ]

### I. INTRODUCTION

We have investigated the electric dipole giant resonance of  $^{11}\text{B}$  by means of inelastic electron scattering. A similar investigation of  $^{13}\text{C}$  has been made by Bergstrom *et al.*<sup>1</sup> Theoretical calculations of the electric dipole giant resonance of  $^{11}\text{B}$  have been made by Fraser and Spicer<sup>2</sup> who considered two hole- one particle excitations. Their calculations are similar to earlier calculations for  $^{13}\text{C}$  by Easlea<sup>3</sup> who considered two particle- one hole excitations. These predictions for  $^{11}\text{B}$  and  $^{13}\text{C}$  show a strong resemblance, including a comparable isospin splitting of the giant resonance into  $T = \frac{1}{2}$  and  $T = \frac{3}{2}$  components. In Easlea's calculation the excited hole can couple also to the  $^{13}\text{C}$  valence  $p_{1/2}$  neutron to produce a  $2^+$  vibration of the  $^{12}\text{C}$  core, which in turn couples to the excited nucleon to form the  $T = \frac{1}{2}$  "pygmy" resonance.<sup>4</sup> The results of Bergstrom *et al.*<sup>1</sup> are in reasonable agreement with Easlea's predictions.

Although there have been no previous investigations of the  $^{11}\text{B}$  giant resonance by electron scattering, there have been several photonuclear investigations. The  $(\gamma, n)$  cross section has been measured by Hayward and Stovall,<sup>5</sup> and by Hughes and Muirhead,<sup>6</sup> and the  $(\gamma, p)$  cross section has been measured by Sorokin, Shevchenko, and Yur'ev.<sup>7</sup> These measurements show the  $^{11}\text{B}$  giant resonance to have more peaks than have been found in  $(\gamma, n)$  and  $(\gamma, p)$  studies<sup>8, 4</sup> of the  $^{12}\text{C}$  and  $^{13}\text{C}$  giant resonances.

We have measured the  $^{11}\text{B}(e, e')$  spectra up to an excitation energy of 32 MeV and have found only a

broad and relatively unstructured giant resonance in contrast to the photonuclear results. This is also in contrast to the  $^{13}\text{C}(e, e')$  results.<sup>1</sup>

The momentum transfer  $q$  was held approximately constant at  $0.4 \text{ fm}^{-1}$  so that the cross sections could be separated into longitudinal and transverse components. A radiative unfolding procedure was used in obtaining the continuum cross section above particle thresholds. In addition, bound state cross sections were obtained for the states at 2.12, 4.44, 5.02, 8.57, and 8.93 MeV. Reduced radiative transition probabilities for excitations of these states from the ground state were obtained after the cross sections were separated into their longitudinal and transverse components. These bound state results are in good agreement with previous measurements. Above threshold, a mixed  $M1$ - $E2$  transition was observed at 13.0 MeV and evidence of a broad complex of  $M1$  and/or  $M2$  resonances was seen at 15.5 MeV.

### II. EXPERIMENT AND ANALYSIS

The experiment was performed at the 140 MeV electron linear accelerator facility at the National Bureau of Standards. Four incident energies  $E_0$  and two scattering angles  $\theta$  were used: 77.0 MeV ( $75^\circ$ ), 90.0 MeV ( $75^\circ$ ), 52.3 MeV ( $145^\circ$ ), and 58.9 MeV ( $145^\circ$ ). For the 77.0 and 52.3 MeV runs we observed excitation energies up to 32 MeV; for the 90.0 MeV run, up to 23 MeV; and for the 58.9 MeV run, up to 18.5 MeV. Scattered electrons passed through a double focusing magnetic spectrometer<sup>9</sup> and were detected by a triple coincidence hodoscope in the spectrometer focal plane.<sup>10</sup> The

hodoscope contains: first, a ladder of 48 small, lithium-drifted silicon detectors which define the electron momentum; secondly, three parallel, coplanar plastic scintillators which define the transverse position of the scattered electron; and finally a single large backup plastic scintillator. The two outer transverse position detectors distinguish background particles from electrons which originate from the target and pass through the spectrometer freely without rescattering.

Our target consisted of 98.5% isotopically pure  $^{11}\text{B}$  powder which had been compacted into a  $100\text{ mg/cm}^2$  disk by subjecting it to a pressure of 4 kilobars. It was then sandwiched between two  $2.5\text{ mg/cm}^2$  thick  $^9\text{Be}$  foils for support and was oscillated in the beam to average out the target density variations. A beryllium target was used concurrently for subtraction purposes, and  $^{12}\text{C}$  elastic data were taken to check the  $^{11}\text{B}$  elastic cross section parameters.

The incident electron beam current was monitored continuously by a Faraday cup for the  $75^\circ$  runs. In order to reduce the neutron background, we

moved the Faraday cup out of the beam for the  $145^\circ$  runs and used a toroidal ferrite current monitor upstream of the target. Since the ferrite was not an absolute device, we calibrated it periodically against the Faraday cup.<sup>11</sup>

The raw data were corrected for spectrometer dispersion, detector efficiencies, and dead time losses. Instrumental and room backgrounds were removed by subtracting the triple coincidences which involved the outer transverse position detectors from those which involved the center detector. The background spectrum due to the beryllium windows was subtracted after convoluting it with the  $^{11}\text{B}$  elastic peak shape in order to simulate straggling. A typical corrected  $^{11}\text{B}$  spectrum is shown in Fig. 1.

Inelastic peak areas were measured relative to the observed elastic peak area, obtained by integrating the elastic peak out to a cutoff energy  $\Delta E$  and applying the Schwinger, Bethe-Heitler, and straggling corrections.<sup>12</sup> Cross sections were then produced by normalization to the calculated value of the elastic cross section computed with

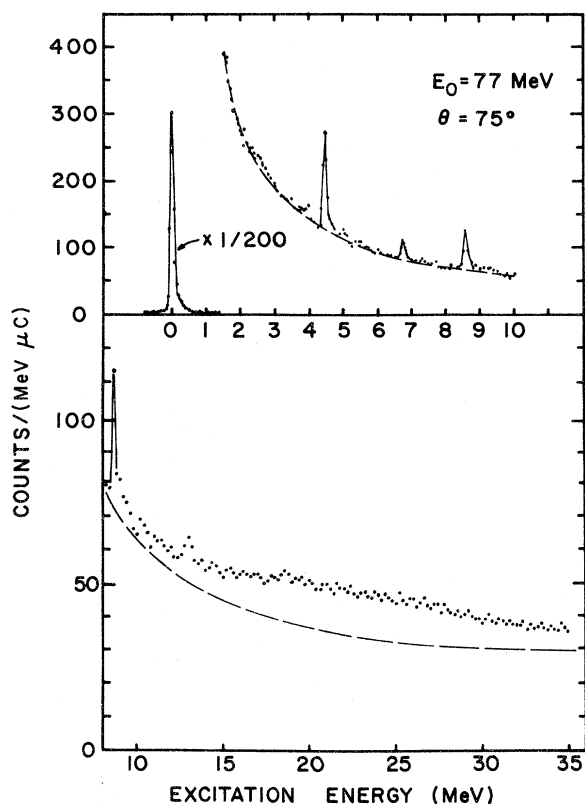


FIG. 1. The energy spectrum of electrons of incident energy 77 MeV scattered through an angle of  $75^\circ$  from a  $100\text{ mg/cm}^2$  thick  $^{11}\text{B}$  target. The dashed curve is the calculated elastic radiation tail.

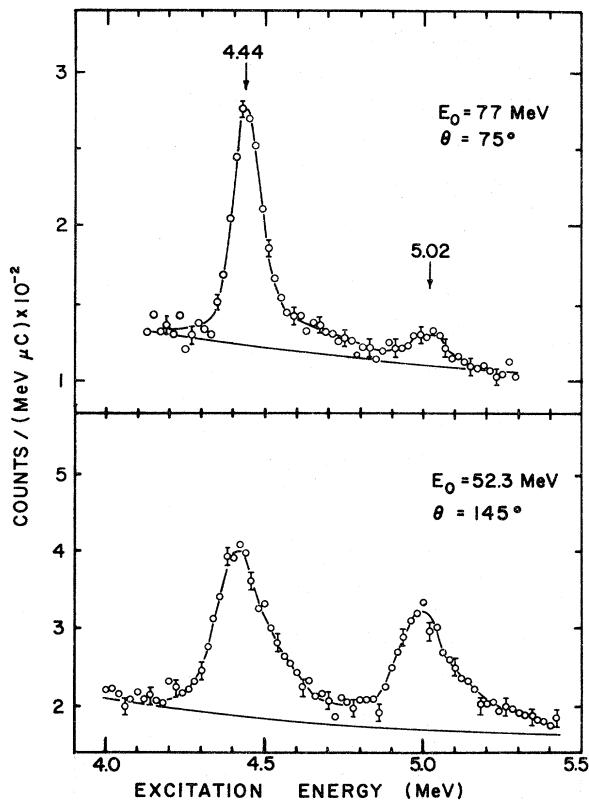


FIG. 2. A least-squares fit to the peaks at 4.44 and 5.02 MeV of a phenomenological radiation tail under scaled elastic peak shapes. The same momentum transfer was used in each case.

the Rawitscher-Fischer phase shift code,<sup>13</sup> using the parameters  $c=2.17$  fm and  $t=2.19$  fm<sup>14</sup> in a two-parameter Fermi model.

#### A. Bound states

The methods by which the inelastic cross sections were obtained depended upon whether the peaks were located above or below the particle emission thresholds. The bound states have very narrow intrinsic widths, but their corresponding inelastic peaks are broadened mainly by the energy spread in the beam and by straggling in the target. The inelastic cross sections  $d\sigma/d\Omega$  for the bound states were obtained by scaling<sup>15</sup> the observed elastic peak shape to the inelastic peaks superimposed on an underlying phenomenological radiation tail. The results of fitting the peaks at 4.44 and 5.02 MeV are shown in Fig. 2.

The square of the inelastic form factor at a momentum transfer  $q$  is defined as

$$|F_{\text{in}}(q)|^2 = (d\sigma/d\Omega)/\sigma_{\text{Mott}},$$

where  $\sigma_{\text{Mott}}$  is the Mott cross section for scattering from a point charge  $Ze$ . In the first Born approximation,  $|F_{\text{in}}|^2$  can be separated into a Coulomb part  $|F_C|^2$ , and transverse electric  $|F_T^E|^2$  and magnetic  $|F_T^M|^2$  parts by using the equation<sup>16</sup>

$$|F_{\text{in}}|^2 = \left(\frac{q_\mu}{q}\right)^4 |F_C|^2 + \left[\frac{1}{2}\left(\frac{q_\mu}{q}\right)^2 + \tan^2\left(\frac{1}{2}\theta\right)\right] \times [ |F_T^E|^2 + |F_T^M|^2 ],$$

and by making measurements at the same  $q$ , but at different  $E_0$  and  $\theta$ .

The reduced transition probabilities for excitation from the ground state,  $B(EL\uparrow)$  and  $B(ML\uparrow)$ , are related in the first Born approximation to the inelastic form factors for small  $q$  by the equations<sup>17</sup>

$$|F_C(q)|^2 = \frac{4\pi}{Z^2} \frac{q^{2L}}{[(2L+1)!!]^2} B(EL\uparrow) \times \left[ 1 - \frac{q^2}{2(2L+3)} R_{\text{tr}}^2(CL) \right]^2$$

and

$$|F_T^M(q)|^2 = \frac{4\pi}{Z^2} \frac{q^{2L}}{[(2L+1)!!]^2} \frac{L+1}{L} B(ML\uparrow) \times \left[ 1 - \frac{q^2}{2(2L+3)} \frac{L+3}{L+1} R_{\text{tr}}^2(ML) \right]^2,$$

where  $L$  is the transition multipolarity and  $R_{\text{tr}}$  the transition radius. For the range of  $q$  used in this experiment, we have estimated  $|F_T^E|^2$  from the equation

$$|F_T^E(q)|^2 = \frac{L+1}{L} \left(\frac{\omega}{q}\right)^2 |F_C|^2.$$

The partial width for excitation from the ground state is defined by

$$\Gamma_\gamma^0 = 8\pi\alpha \frac{(2J_i+1)}{(2J_f+1)} \frac{L+1}{L} \times \frac{\omega^{2L+1}}{[(2L+1)!!]^2} B\left(\frac{E}{M}L\uparrow\right),$$

where  $\omega$  is the excitation energy. In fitting to obtain  $B(EL)$  and  $B(ML)$ , we used Spamer's<sup>17</sup> values of the transition radii.

#### B. Continuum states

The continuum states beyond the  $(\gamma, p)$  and  $(\gamma, n)$  thresholds, 11.23 and 11.46 MeV, respectively, have large natural widths which are no longer negligible compared with the beam energy spread, and the peak fitting procedure which uses the phenomenological radiation tail as previously described cannot be applied. Instead, a radiative unfolding technique was used to correct for those electrons which had been degraded in energy by bremsstrahlung emission before or after scattering, either in the field of the same nucleus in which a large angle scattering takes place, or in the field of another nucleus. The first of these processes is much more important for target thicknesses of the order of 0.01 radiation lengths because the count rate from this process is proportional to  $t$ , the target thickness in radiation lengths, while that from the second process is proportional to  $t^2$ . For the first process,  $d^2\sigma/d\Omega dE$  is obtained by integrating the Bethe-Heitler cross section over all photon angles. For this we have used the elastic scattering tail formula of Maximon and Isabelle<sup>18</sup> which was separated into two parts: a peaking term which contributes no less than 80% to the cross section at our energies and angles, and a "background" term which includes several integral expressions. The first three integrals in the background term were neglected for the forward angle runs since their sum amounted to less than 0.1% of the radiative cross section. For backward angles where the sum at its largest value was just under 1%, we approximated these integrals by quadratic functions with fitted coefficients in order to save computing time. For the second bremsstrahlung process, we used the expression of Isabelle and Bishop.<sup>12</sup>

The large radiation tail associated with elastic scattering, as shown in Fig. 1, was subtracted from the spectrum before radiative unfolding was carried out. A harmonic oscillator charge form factor with an rms radius<sup>19</sup> of 2.42 fm was used for computational convenience in the calculation of the elastic tail for all points beyond the cutoff

energy which defines the elastic peak. The Born approximation elastic cross section calculated with this form factor agreed with the phase shift method mentioned earlier to better than 2.5%.

A bin-by-bin radiative unfolding of the remaining inelastic spectrum was performed by first applying inelastic Schwinger, Bethe-Heitler, and ionization corrections<sup>12</sup> to the counts in the first bin at the highest electron energy at which the unfolding began. The corrected counts represented the cross section of that bin. The inelastic radiative tail, based on another formula by Maximon and Isabelle,<sup>20</sup> was normalized to the counts in this bin and subtracted from all subsequent bins in the spectrum. Two approximations were made at this juncture: (i) only the peaking term was used, and (ii) phenomenological inelastic form factors were used. For any given bin in the spectrum, contributions from inelastic tails due to all previous bins were removed before applying

the radiative and ionization corrections. The radiatively corrected spectra are shown in Fig. 3.

### III. RESULTS

#### A. Continuum

All four spectra of Fig. 3 show little sharp structure above the particle emission thresholds with the exception of a pronounced peak about 500 keV wide at  $13.0 \pm 0.1$  MeV, which may have been observed earlier.<sup>21-23</sup> In Fig. 4 an assumed linear background has been subtracted from this peak in all four spectra and the resultant cross section profiles have been overlaid. The peak has comparable longitudinal and transverse form factors in this range of  $q$  and the apparent shifting of the maximum indicates that perhaps several states have been excited. In a recent inelastic neutron scattering experiment,<sup>24</sup> a  $J^\pi$  value of  $\frac{3}{2}^-$  was assigned to a state at 13.12 MeV and  $\frac{5}{2}^+$  to one

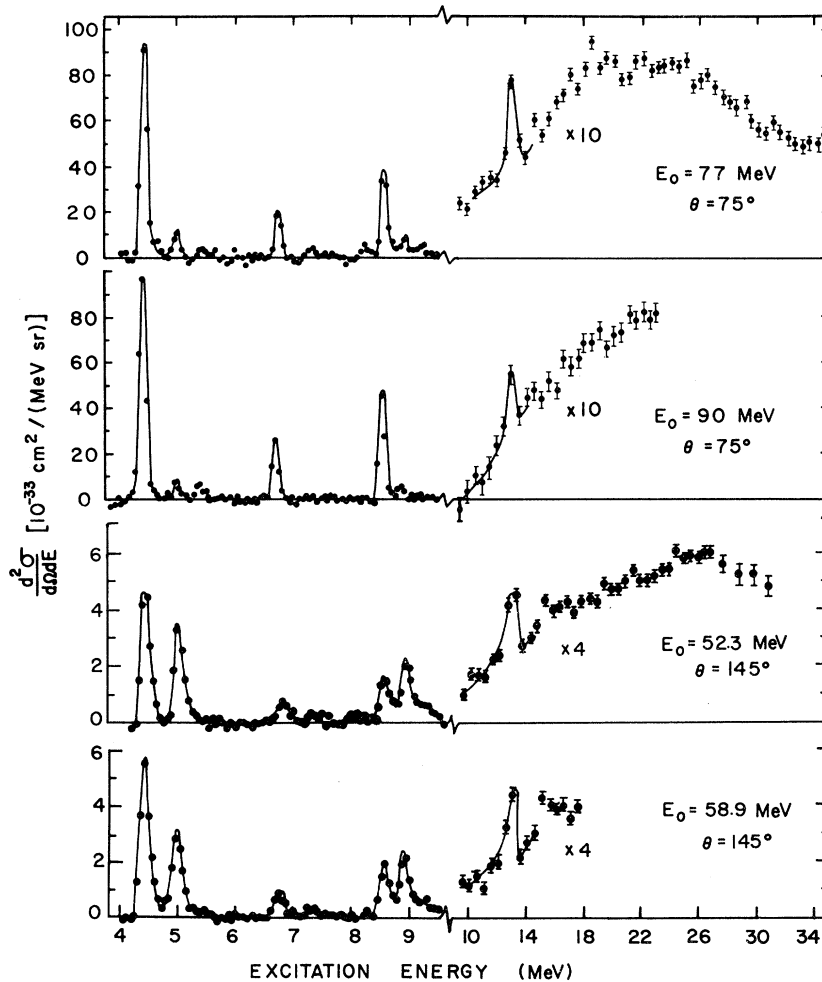


FIG. 3. The radiatively unfolded spectra.

at 13.17 MeV. It is not likely that we have excited the former state because high multipolarity excitations are suppressed at our relatively low momentum transfers. The latter could go by an  $E1$  or  $M2$ . On the other hand, Goosman, Adelberger, and Snover<sup>22</sup> assigned an isospin of  $\frac{3}{2}$  and  $J^\pi = \frac{1}{2}^-$  to a state at 12.91 MeV in a proton capture reaction. They obtained a value of  $29 \pm 8$  eV for the partial width for decay to the ground state, based upon an updated measurement<sup>25</sup> of the half-life for  $^{10}\text{Be}$ . By assuming  $J^\pi = \frac{1}{2}^-$  and an  $M1$  excitation for the transverse component of the state, we obtain a value of  $36 \pm 7$  eV which is consistent with Goosman's result. Our slightly higher result may indicate the presence of transverse strength other than  $M1$ , or excitation of the nearby  $\frac{5}{2}^+$  state. If  $J^\pi = \frac{3}{2}^-$ , then  $\Gamma_\gamma = 18 \pm 4$  eV, in agreement with the calculation of Cohen and Kurath.<sup>26</sup>

The radiatively unfolded continuum data have been further analyzed by separating the longitudinal  $|W_L(q, \omega)|^2$ , and transverse  $|W_T(q, \omega)|^2$ , components of the square of the differential form factor<sup>27</sup>

$$|W(q, \omega)|^2 = (d^2\sigma/d\Omega dE)/\sigma_{\text{Mott}}.$$

For each pair of experimental continuum data sets having the same nominal  $q$ , we considered the variation of  $q$  with excitation energy  $\omega$  by summing the spectrum into variable width bins such that the fractional spread in both  $q$  and  $\omega$  was about the same. For the 77.0 and 52.3 MeV data, the  $q$ 's matched closely only for  $\omega$  from about 9 to 13 MeV. At 30 MeV a bin width of 4 MeV was imposed. The absence of strong minima in the spectra prevented the placement of bin edges as Bergstrom *et al.*<sup>1</sup> were able to do for  $^{13}\text{C}$ . A point-for-point comparison of the longitudinal and transverse differential form factors, derived from the 77.0 and 52.3 MeV data, is shown in Fig. 5. Over the excitation energies indicated,  $q$  varies by 20%. The maximum of  $W_L^2$  occurs some 6 MeV lower than that of  $W_T^2$  and it is about three times larger. Also shown in Fig. 5 are estimates of  $W_T^2$  deduced from  $W_L^2$  by using

$$|W_T(q, \omega)|^2 \approx \frac{L+1}{L} \left(\frac{\omega}{q}\right)^2 |W_L(q, \omega)|^2, \quad (1)$$

which is derived from Siegert's theorem.<sup>16</sup> These estimates are smaller than the measured values but have a similar dependence on excitation energy. The  $W_T^2$  values obtained from Eq. (1) will only describe the electric non-spin-flip components contained in the transverse excitations, and the difference between these and the experimentally separated  $W_T^2$  could be attributed to the existence

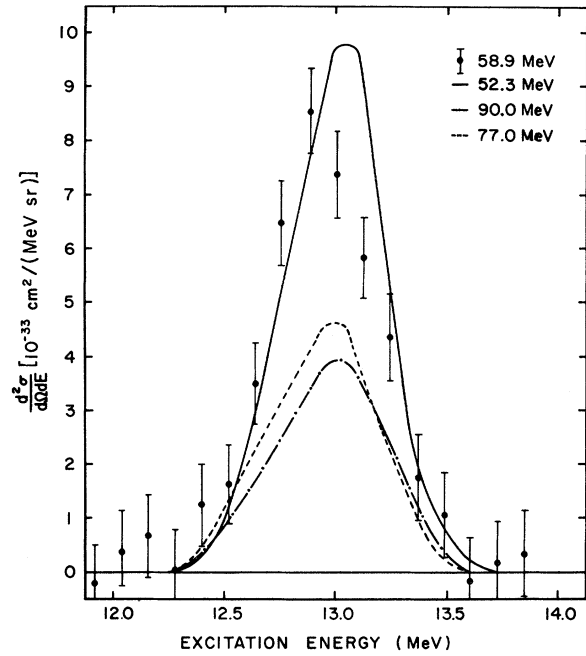


FIG. 4. Overlaid peak profiles of the 13.0 MeV peak after a linear background has been subtracted. The shapes from the 77.0, 90.0, and 52.3 MeV spectra are represented by smooth curves through the data points with uncertainties comparable to those shown for the 58.9 MeV data.

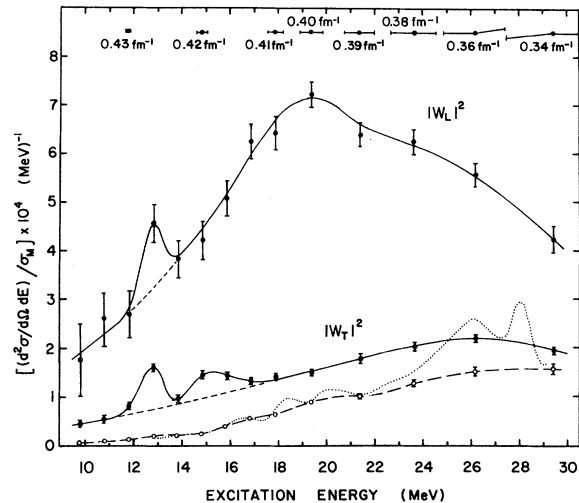


FIG. 5. Separated longitudinal  $W_L^2$ , and transverse  $W_T^2$ , differential form factors squared (solid circles) and the estimated non-spin-flip transverse component using Siegert's theorem (open circles). The transformed photoabsorption cross section is shown approximated by  $^{11}\text{B}(\gamma, n)$  data (Refs. 5 and 6) normalized to 63% of the TRK dipole sum rule limit (dotted line). The indicated errors are purely statistical.

of electric spin-flip components or magnetic transitions.

A comparison of  $W_T^2$  and photoabsorption data was made by assuming that the  $^{11}\text{B}$  giant resonance excited state form factors are closely related to corresponding states in  $^{12}\text{C}$ . In the absence of a direct measurement of the total absorption cross section, we have approximated it by the  $^{11}\text{B}(\gamma, n)$  cross section<sup>5,6</sup> normalized to the fraction<sup>28</sup> of the Thomas-Reich-Kuhn (TRK) dipole sum rule limit exhausted in  $^{12}\text{C}$  within the excitation range up to 30 MeV. The photoabsorption cross section was transformed to a differential form factor at the  $q$  values in this experiment, using weighted form factors for particle-hole configurations which seemed to describe<sup>29</sup> the  $q$  dependence of the integrated dipole strength in  $^{12}\text{C}$ .

The transformed photoabsorption cross section in Fig. 5 rises with excitation energy to follow the Siegert theorem estimate until about 22 MeV, but it departs at higher energies to agree with the measured transverse form factor. Much the same results were obtained by approximating the photoabsorption form factors from a summation of  $(\gamma, n)$  and  $(\gamma, p)$  cross sections. However, peaks from the  $(\gamma, p)$  data<sup>7</sup> are not observed in the present measurement. The region above approximately 22 MeV thus appears to consist predominantly of  $E1$  transitions that produce the dipole giant resonance in the photoreactions. A considerable fraction of these transitions involve a large spin-flip

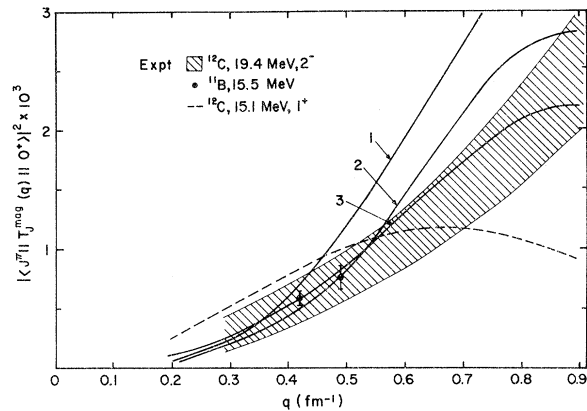


FIG. 6. Comparison of transition matrix elements obtained from the 15.5 MeV structure in the present data with the 19.4 MeV,  $2^-$  and 15.1 MeV,  $1^+$  states in  $^{12}\text{C}$ . The cross-hatched region represents the trend of experimental data for the  $2^-$  state and the solid lines indicate predictions based on (1) the Goldhaber-Teller model, (2) the particle-hole model and (3) the p-h model with coupled surface vibrations (see Ref. 16). The dashed line shows the  $1^+$  state obtained by a fit of a single particle shell model expression to experiment (Ref. 29).

TABLE I. Bound state cross sections.

Level (MeV)	$E_0$ (MeV)	$\theta$ (deg)	$\frac{d\sigma}{d\Omega}$ ( $\text{cm}^2/\text{sr}$ )
2.12	77	75	$(3.38 \pm 1.6) \times 10^{-33}$
	90	75	$(4.45 \pm 1.7) \times 10^{-32}$
	52.3	145	$(4.95 \pm 0.9) \times 10^{-33}$
	58.9	145	$(5.38 \pm 1.9) \times 10^{-33}$
4.44	77	75	$(1.53 \pm 0.06) \times 10^{-31}$
	90	75	$(1.79 \pm 0.08) \times 10^{-31}$
	52.3	145	$(1.59 \pm 0.07) \times 10^{-32}$
	58.9	145	$(1.46 \pm 0.06) \times 10^{-32}$
5.02	77	75	$(1.98 \pm 0.03) \times 10^{-32}$
	90	75	$(1.42 \pm 0.52) \times 10^{-32}$
	52.3	145	$(1.05 \pm 0.05) \times 10^{-32}$
	58.9	145	$(7.89 \pm 0.42) \times 10^{-33}$
8.57	77	75	$(6.15 \pm 0.33) \times 10^{-32}$
	90	75	$(6.78 \pm 0.30) \times 10^{-32}$
	52.3	145	$(4.55 \pm 0.49) \times 10^{-33}$
	58.9	145	$(4.89 \pm 0.36) \times 10^{-34}$
8.93	77	75	$(1.12 \pm 0.24) \times 10^{-32}$
	90	75	$(1.02 \pm 0.19) \times 10^{-32}$
	52.3	145	$(5.98 \pm 0.52) \times 10^{-33}$
	58.9	145	$(5.43 \pm 0.38) \times 10^{-33}$

component which can be attributed to  $(1p_{3/2})^{-2}1d_{3/2}$  excitations. Below 22 MeV the accord of the transformed photodata with the Siegert theorem estimate indicates that there is little  $E1$  spin-flip component. This in turn implies that the admixture of configurations assumed for the transformation of the photoreaction data is probably incorrect. We find that transforming the photodata assuming a  $(1p_{3/2})^{-2}1d_{5/2}$  configuration alone will give reasonable agreement with the Siegert theorem estimate in this region. Although the hole excitation  $(1s_{1/2})^{-1}$  does not seem to contribute in a large way to the dipole transition strength, there is evidence in the  $^9\text{Be}(d, \gamma_0)$  data of Battleson and McDaniel<sup>30</sup> of at least two relatively narrow  $T = \frac{1}{2}$  states involving this configuration which could be spread over many such levels around 18 MeV. We note that this particular excitation is not possible in  $^{13}\text{C}$ .

In this lower excitation region, the experimental values of  $W_T^2$  are considerably larger than those estimated from Eq. (1) or photoabsorption. This suggests the presence of magnetic transitions or electric multipoles higher than  $E1$ . In particular, an approximately 3 MeV wide resonance appears only in the transverse curve at 15.5 MeV. It is likely to be dominated by magnetic transitions, in agreement with Kossanyi-Demay and Vanpraet<sup>21</sup> who observed in  $180^\circ$  electron scattering at least two strong states between 14 and 17

TABLE II. Level properties.

Energy (MeV)	$J^\pi, T$	Transitions	$B(\frac{E}{M}L\uparrow)$ ( $e^2 \text{fm}^{2L}$ ) This expt.      Other expts. <sup>a</sup>	This expt.	$\Gamma_\gamma^0 / \Gamma_W$	$\Gamma_\gamma^0$ (eV) Other expts.	Theory <sup>b</sup>
2.12	$\frac{1}{2}^-, \frac{1}{2}$	M1	(6.8 ± 2) × 10 <sup>-3</sup>	0.14 ± 0.04	0.70	0.16 ± 0.02 <sup>a</sup> 0.23 ± 0.09 <sup>c</sup>	0.09–0.11
4.44	$\frac{5}{2}^-, \frac{1}{2}$	M1	(1.20 ± 0.12) × 10 <sup>-2</sup>	0.73 ± 0.07	0.39	0.63 ± 0.07 <sup>a</sup> 0.53 ± 0.21 <sup>c</sup> 0.60 ± 0.20 <sup>d</sup>	0.79–0.81
5.02	$\frac{3}{2}^-, \frac{1}{2}$	E2 M1	21.3 ± 2.0 (1.60 ± 0.16) × 10 <sup>-2</sup>	(2.0 ± 0.2) × 10 <sup>-2</sup> 2.12 ± 0.21	9.7 0.80	(1.71 ± 0.16) × 10 <sup>-2</sup> <sup>a</sup> 1.82 ± 0.08 <sup>a</sup> 2.42 ± 0.76 <sup>d</sup>	1.9–2.0
8.57	$\frac{3}{2}^-, \frac{1}{2}$	M1	(1.7 ± 0.2) × 10 <sup>-3</sup>	0.73 ± 0.07	0.06	0.72 ± 0.30 <sup>a</sup>	0.03–0.17
8.93	$\frac{5}{2}^-, \frac{1}{2}$	E2 M1	9.37 ± 0.15 (9.9 ± 1) × 10 <sup>-3</sup>	0.23 ± 0.03 4.93 ± 0.50	4.2 0.33	0.4 ± 0.1 <sup>a</sup> 4.0 ± 0.6 <sup>a</sup> 5.0 ± 1.2 <sup>d</sup>	3.2–4.6
13.0 <sup>e</sup>	$\frac{1}{2}^-, (\frac{3}{2})$ $\frac{3}{2}^-, (\frac{3}{2})$ $\frac{1}{2}^-, (\frac{3}{2})$ $\frac{3}{2}^-, (\frac{3}{2})$	M1 E2	(7.9 ± 2) × 10 <sup>-3</sup> 3.6 ± 0.5	36 ± 7 18 ± 4 2.2 ± 0.2 1.1 ± 0.1	0.78 0.39 5.0 2.5	29 ± 8 <sup>f</sup>	15–19 17–19

<sup>a</sup> Reference 17.<sup>b</sup> Reference 26. Range of values resulting from different parametrizations of the two-body matrix elements.<sup>c</sup> Reference 31.<sup>d</sup> Reference 21.<sup>e</sup> Above breakup thresholds.<sup>f</sup> References 22 and 25.

MeV at a resolution close to 1 MeV. The form factor for the 15.5 MeV resonance has been extracted at two average values of momentum transfer, namely 0.42 and 0.49 fm<sup>-1</sup>, after subtraction of a linear background assumed to account for contributions of underlying electric multipole states and a smooth quasielastic scattering continuum. The two values normalized by  $(2J_i + 1)$ , where  $J_i = \frac{3}{2}$  is the ground state spin of <sup>11</sup>B, are compared in Fig. 6 with transition matrix elements of the 2<sup>-</sup> *M2* giant resonance state in <sup>12</sup>C at 19.4 MeV and the 1<sup>+</sup> single particle state at 15.1 MeV.<sup>16</sup> The present data are not sufficient to make a choice between *M1* and *M2* for the 15.5 MeV region in <sup>11</sup>B on the basis of this comparison between these two multipole transitions in <sup>12</sup>C. If the resonance were predominantly *M1*, it represents about 75% of the transition strength contained in the <sup>12</sup>C 15.1 MeV state. Measurements at higher *q* are needed to clarify the character of this resonance.

#### B. Bound states

The measured bound state cross sections are given in Table I, and the extracted quantities are summarized and compared with other works in Table II. The measured *M1* excitation widths from the ground state,  $\Gamma_\gamma^0(M1)$ , of the 2.12, 4.44, 5.02, and 8.93 MeV states agree with previous measurements by Spamer,<sup>17</sup> Kossanyi-Demay and Vanpraet,<sup>21</sup> and by Saito,<sup>31</sup> as well as with the calculation of Cohen and Kurath.<sup>26</sup> Each of these states has a large branching ratio for decay to the ground state.<sup>32</sup> The states at 5.02 and 8.93 MeV both have, within statistics, zero longitudinal strength in the form factor at these momentum transfers. It is not clear which of the states in the calculation<sup>26</sup> of Cohen and Kurath corresponds to the 8.57 MeV state observed in this experiment. We find that of the bound states studied, the 8.57 MeV state has the largest proportion of transverse electric transition strength (~30%). The states at 6.74 and 6.79 MeV were not sufficiently resolved to be analyzed.

#### IV. SUMMARY

The dipole giant resonance is shown to be distributed over a wide region of excitation energy. However, the longitudinal and transverse components of the differential cross section are found to peak at different energies, at 19 and 26 MeV, respectively. The comparison of mea-

sured and estimated values of  $W_T^2$  indicates that *E1* excitations involving the  $(1p_{3/2})^{-2}1d_{5/2}$  configuration may largely account for the longitudinal component. The transverse *E1* component is probably dominated by the same configuration below 22 MeV, but at higher energies near the maximum in  $W_T^2$ , a comparable contribution is provided by the spin-flip  $(1p_{3/2})^{-2}1d_{3/2}$  configuration. This distribution of configuration strength is consistent with the calculation of Fraser and Spicer.<sup>2</sup>

Little can be determined directly about the isospin character of the giant resonance. Donnelly points out that the *T*=1 states in <sup>12</sup>C should be strongly transverse due to the large isovector magnetic moment compared to the isoscalar magnetic moment. Since only *T*=1, 1<sup>-</sup> states in <sup>12</sup>C can couple to the *T*= $\frac{1}{2}$ ,  $1p_{3/2}$  hole to form *T*= $\frac{3}{2}$  dipole states in <sup>11</sup>B, these latter states might be expected to be strongly transverse also and contribute a major proportion of excitation strength to  $W_T^2$  estimated from the photoabsorption cross section. Since both isovector and isoscalar terms in the transition operator will allow *T*= $\frac{1}{2}$  *E1* states in <sup>11</sup>B, the *T*= $\frac{1}{2}$  excitation strength can be distributed through both  $W_L^2$  and  $W_T^2$ . While not conclusive, deexcitation  $\gamma$ -ray data,<sup>33</sup> and radiative capture experiments<sup>34, 35</sup> which populate *T*= $\frac{1}{2}$  states in mass-11 nuclei, suggest that much of the *T*= $\frac{1}{2}$  strength does lie below 22 MeV. Consequently, the separation of the maxima in  $W_L^2$  and  $W_T^2$  may be indicative of the existence of isospin splitting of the dipole giant resonance in <sup>11</sup>B. The uncertainty in the extent of isospin splitting would be compounded by the spreading of strength within each component to increase the overlap.

It is noticeable that the giant resonance observed by electron scattering is smoother than those similarly observed in <sup>12</sup>C and <sup>13</sup>C.<sup>1</sup> This could be due to a variety of causes including, perhaps, a distribution of strength due to complicated configurations resulting from the coupling of surface deformations to the dipole excitations.<sup>36</sup> While the  $(1s_{1/2})^{-1}$  hole excitation does not appear to have much *E1* strength associated with it, it could allow a greater degree of core deformation than may be possible in <sup>12</sup>C and <sup>13</sup>C.

We wish to acknowledge the services of the National Bureau of Standards linac operations staff and the University of Massachusetts Computing Center.



- <sup>†</sup>Work supported in part by the Office of Naval Research under Contract No. ONR N00014-67-A-0230-0009.
- <sup>1</sup>J. C. Bergstrom, H. Crannell, F. J. Kline, J. T. O'Brien, J. W. Lightbody, and S. P. Fivozinsky, *Phys. Rev. C* **4**, 1514 (1971).
- <sup>2</sup>R. F. Fraser and B. M. Spicer, *Austr. J. Phys.* **26**, 7 (1973).
- <sup>3</sup>B. R. Easlea, *Phys. Lett.* **1**, 163 (1962).
- <sup>4</sup>B. C. Cook, *Phys. Rev.* **106**, 300 (1957).
- <sup>5</sup>E. Hayward and T. Stovall, *Nucl. Phys.* **69**, 241 (1965).
- <sup>6</sup>R. J. Hughes and E. G. Muirhead, *Nucl. Phys.* **A215**, 147 (1973).
- <sup>7</sup>Yu. I. Sorokin, V. G. Shevchenko, and B. A. Yur'ev, *Yad. Fiz.* **9**, 254 (1969) [transl.: *Sov. J. Nucl. Phys.* **9**, 149 (1969)].
- <sup>8</sup>B. C. Cook, J. E. E. Baglin, J. W. Bradford, and J. E. Griffin, *Phys. Rev.* **143**, 724 (1966).
- <sup>9</sup>S. Penner and J. W. Lightbody, in *Proceedings of the International Symposium on Magnet Technology, Stanford, Calif., 1965*, edited by H. Brechma and M. S. Gordon (NBS, U.S. Dept. of Commerce, Washington, D. C., 1966), p. 154, CONF-650922.
- <sup>10</sup>J. K. Whittaker, *IEEE Trans. Nucl. Sci.* **19**, 444 (1972).
- <sup>11</sup>J. S. Pruitt, *Nucl. Instrum. Methods* **100**, 433 (1972).
- <sup>12</sup>D. B. Isabelle and G. R. Bishop, *Nucl. Phys.* **45**, 209 (1963).
- <sup>13</sup>C. R. Fischer and G. H. Rawitscher, *Phys. Rev.* **135**, B377 (1964).
- <sup>14</sup>H. R. Collard, L. R. B. Elton, and R. Hofstadter, in *Landolt-Börnstein Numerical Data and Functional Relationships in Science and Technology*, edited by K. H. Hellwege and H. Schopper (Springer-Verlag, Berlin, 1967), New Series, Group I, Vol. 2.
- <sup>15</sup>J. F. Zeigler and G. A. Peterson, *Phys. Rev.* **165**, 1337 (1968).
- <sup>16</sup>H. Überall, *Electron Scattering from Complex Nuclei* (Academic, New York and London, 1971).
- <sup>17</sup>E. Spamer, *Z. Phys.* **191**, 24 (1966); E. Spamer and H. Artus, *ibid.* **198**, 445 (1967).
- <sup>18</sup>L. C. Maximon and D. B. Isabelle, *Phys. Rev.* **133**, B1344 (1964).
- <sup>19</sup>T. Stovall, J. Goldenberg, and D. B. Isabelle, *Nucl. Phys.* **86**, 225 (1966).
- <sup>20</sup>L. C. Maximon and D. B. Isabelle, *Phys. Rev.* **136**, B674 (1964).
- <sup>21</sup>P. Kossanyi-Demay and G. J. Vanpraet, *Nucl. Phys.* **81**, 229 (1966).
- <sup>22</sup>D. R. Goosman, E. G. Adelberger, and K. A. Snover, *Phys. Rev. C* **1**, 123 (1970).
- <sup>23</sup>R. D. Edge and G. A. Peterson, *Phys. Rev.* **128**, 2750 (1962).
- <sup>24</sup>S. L. Hausladen, C. E. Nelson, and R. O. Lane, *Nucl. Phys.* **A217**, 563 (1973).
- <sup>25</sup>D. R. Goosman and R. W. Kavanagh, *Phys. Rev. C* **7**, 1717 (1973).
- <sup>26</sup>S. Cohen and D. Kurath, *Nucl. Phys.* **73**, 1 (1965).
- <sup>27</sup>A. Yamaguchi, T. Terasawa, K. Nakahara, and Y. Torizuka, *Phys. Rev. C* **3**, 1750 (1971).
- <sup>28</sup>E. Hayward, NBS Monograph No. 118 (1970).
- <sup>29</sup>T. W. Donnelly, *Phys. Rev. C* **1**, 833 (1970).
- <sup>30</sup>K. Battleson and D. K. McDaniels, *Phys. Rev. C* **4**, 1601 (1971).
- <sup>31</sup>T. Saito, *J. Phys. Soc. Jpn.* **35**, 1 (1973).
- <sup>32</sup>F. Ajzenberg-Selove and T. Lauritsen, *Nucl. Phys.* **A114**, 1 (1968).
- <sup>33</sup>B. H. Patrick, H. A. Medicus, G. K. Mehta, E. M. Bowey, and D. B. Gayther, *Phys. Lett.* **34B**, 488 (1971).
- <sup>34</sup>W. Del Bianco, P. Boucher, S. Kundu, and B. Rouben, *Can. J. Phys.* **52**, 92 (1974).
- <sup>35</sup>H. M. Kuan, M. Hasinoff, W. J. O'Connell, and S. S. Hanna, *Nucl. Phys.* **A151**, 129 (1970).
- <sup>36</sup>H. Überall, *Phys. Rev. Lett.* **17**, 1292 (1966).